Water Science and Engineering 2019, 12(1): 62−72

HOSTED BY

ELSEVIER

Available online at www.sciencedirect.com

Water Science and Engineering

journal homepage: http://www.waterjournal.cn

Computational investigation of hydraulic performance variation with geometry in gabion stepped spillways

Dominic E. Reeve*, Ali Adel Zuhaira, Harshinie Karunarathna

College of Engineering, Swansea University, Swansea SA2 8PP, UK

Received 18 May 2018; accepted 3 January 2019
Available online 8 April 2019

Abstract

Over recent years, there has been a clear increase in the frequency of reported flooding events around the world. Gabion structures offer one means of flood mitigation in dam spillways. These types of structures provide an additional challenge to the computational modeller in that flow through the porous gabions must be simulated. We have used a computational model to investigate the flow over gabion stepped spillways. The model was first validated against published experimental results. Then, gabion stepped spillways with four different step geometries were tested under the same conditions in order to facilitate inter-comparisons and to choose the best option in terms of energy dissipation. The results show that normal gabion steps can dissipate more energy than overlap, inclined, and pooled steps. An intensive set of tests with varying slope, stone size, and porosity were undertaken. The location of the inception point and the water depth at this point obtained from this study were compared with those from existing formulae. Two new empirical equations have been derived, on the basis of a regression analysis, to provide improved results for gabion stepped spillways.

Keywords: Computational modelling; Energy dissipation; Gabion stepped spillways; Inception point location; Skimming flow

1. Introduction

Spillways can be defined as structures, located over dams, whose function is to release any excess water during the flooding seasons in order to reduce the probability of having an overtopping failure (Novak et al., 2001). Many materials can be used in the construction of spillways, including roller compact concrete and gabions. Each material has advantages and disadvantages (Boes and Hager, 2003). Energy dissipation can be considered one of the main design elements of stepped spillways because the high energy of the flow can cause many problems at the toe of the structure, such as the formation of scour holes, which can lead to structural failure in spillway foundations. Also, overtopping damage can occur, which can cause significant problems for people in the surrounding areas (Novak et al., 2010).

Chanson (2002) has defined two types of flow over stepped spillways: non-aerated flow and aerated flow. Normally, non-aerated flow takes place along the upper steps of spillways where there is no air entrainment, while aerated flow can be observed along the lower steps where air entrainment occurs (e.g. André and Schleiss, 2004; Chanson, 1994, 1995). For the same geometry, when the discharge increases, the length of the non-aerated zone also increases. Thus, the likelihood of generating cavitation will also increase. As noted by Husain et al. (2013), cavitation can be extremely damaging and even destroy spillways, leading to operational failure of the steps and spillways. The aerated zone can be determined by estimating the location of the inception point, which represents the endpoint for the non-aerated zone and the start of the aerated zone. The inception point is the location where the boundary layer intersects the free surface of the water

This work was supported by the Higher Committee for Education Development (HCED) in Iraq.
* Corresponding author
E-mail address: d.e.reeve@swansea.ac.uk (Dominic E. Reeve).
Peer review under responsibility of Hohai University.

https://doi.org/10.1016/j.wse.2019.04.002

(Chanson, 1994, 1996). Flow over stepped spillways can be classified into three hydraulic regimes: nappe flow, transition flow, and skimming flow (Zhang and Chanson, 2016b).

Traditionally, spillways have been impermeable. However, the use of a permeable layer such as gabions offers a means to improve the hydraulic performance by enhancing energy dissipation. Gabions are containers that can be filled with gravel, cobbles, stones, and rocks, depending on the purpose of construction. Since 1879, gabions have been used in China and Egypt. Gabions have also been used for different purposes such as riverbed protection, bank stabilization, and retaining walls. There are three different types of gabions: basket, mattress, and sack. All of these may be filled with gravel and/or cobble materials (Zhang and Chanson, 2014). The choice of gabion type depends upon the application. For instance, basket gabions are commonly used for stability purposes and to protect river beds and stream banks (Freeman and Fischenich, 2000). A brief discussion of earlier studies conducted on gabion stepped spillways is provided below.

Gabions are one common construction element for spillways in the African Sahel (Peyras et al., 1992). Gabions have been used widely for water structures like small earth dams, retaining walls, intakes, and soil conservation work. Salmasi et al. (2012) stated that there are many benefits from using gabions, such as ease of construction, structural stability, flexibility, and resistance to water load. The resistance to water load is likely to be related to flow through porous media. Porosity can help the water to drain faster and reduce the water load behind the structure (Zhang and Chanson, 2016a). Permeability is known to affect the flow properties of the free surface in many cases (Manes et al., 2009). It has been suggested that related flow mechanisms can play a vital role in increasing or decreasing friction factors, thereby affecting the shear penetration within the permeable bed, which can in turn affect the boundary layer. Hence, increasing the flow resistance may increase energy dissipation due to the momentum exchange between the surface and subsurface flows.

Stephenson (1979) performed a study on energy dissipation over stepped gabions. Different configurations were examined, such as stepped gabions with two to four steps and with four different slopes: 1:1, 1:2, 1:3, and 2:3. The energy dissipation was calculated using the differences in depths between the areas upstream and downstream. The results showed that the relative energy dissipation ranged from 25% to 85%. They also showed that the energy dissipation increased as the number of steps increased to three, but then decreased as the number of steps increased further. Concerns about the ability of gabion steps to resist damage under high flows were addressed by the experimental study of Peyras et al. (1992), who showed that gabion stepped weirs can withstand floods up to 3 $m^3/(m \cdot s)$ without any damage. Kells (1994) studied the energy dissipation over a gabion stepped weir as a function of the critical depth at and discharge over the crest. This experimental study used two downstream slopes of 1:1 and 1:2, and the main finding was that 20% of the energy can be dissipated due to the through-flow. Moreover, no significant differences were noticed in the energy dissipation when the slopes changed. It is important to note that the number of the steps in the previous studies affected the energy dissipation results more than the spillway slope. Therefore, more research is required to investigate the impact of the number of steps.

The sensitivity of the hydraulic performance to the characteristics of the material contained in gabions was investigated experimentally by Chinnarasri et al. (2008). They used three stone types: (1) crushed stone of about 25−35 mm in diameter; (2) rounded stone of about 25−35 mm in diameter; and (3) crushed stone of about 50−70 mm in diameter. The results showed that the energy dissipation ratios over gabion stepped weirs were greater than those over the corresponding impermeable stepped weirs by nearly 7%, 10%, and 14% for weir slopes of 30°, 45°, and 60°, respectively. Consequently, the outlet velocity was lower. Moreover, the results showed that both the stone size and stone shape had a small effect on the energy loss and flow velocity compared to the weir slope. The pressure on the step face of gabion stepped weirs was less than that on the horizontal step due to the dampening influence of filled stones. The average pressure difference was approximately 29%. More recently, Wüthrich and Chanson (2014) carried out a laboratory study to investigate the hydraulic characteristics of flow, such as flow patterns, air-water flow properties, and energy dissipation over normal and gabion stepped spillways with a 1:2 slope and a 0.1-m step height. This study was conducted with a wide range of flow rates in order to investigate nappe, transition, and skimming flows. They found that large velocities could be observed at the downstream end of gabion stepped spillways, as well as low rates of energy dissipation over gabion steps in comparison to smooth impervious steps. It can be concluded that there are many parameters with impacts on the performance of gabion stepped spillways, such as the size of stones, water flow conditions, and the air-flow entrainment. However, at present, there is no clear picture of which of these parameters has the strongest influence on the efficiency of gabion stepped spillways. Thus, further investigations are needed to determine the essential controlling factors.

It is well established that stepped spillways (gabion or other) have an advantage over non-stepped spillways in terms of reducing cavitation damage due to air entrainment and by improving energy dissipation performance (Husain, 2013). Although there is a well-developed understanding of the performance of normal stepped spillways, the same level of understanding has not been developed for gabion stepped chutes with more complex designs. Moreover, even though stepped spillways have been extensively studied using computational models, detailed numerical modelling studies on gabion stepped spillways have not been recorded. Also, gabion porosity and gabion stone size, both of which affect the flow, need to be investigated in detail in order to demonstrate their impacts on other important parameters, such as the location of the inception point. Finally, finding an optimum gabion stepped spillway design can improve performance and offer an alternative for stepped spillway construction.

In this study, we used a computational model as a *numerical flume* to investigate the performance of gabion stepped

spillways under a range of conditions that covered spillway slope, step geometry, step height, gabion stone size, and porosity. In Section 2 details of the computational model are described together with some validation results. In Section 3, results of the computations along with discussion of their implications for hydraulic performance are presented, and the computational results obtained in this study are compared with those of some existing empirical equations for estimation of the location of the inception point and water depth at that point. Finally, two new equations are proposed for gabion stepped spillways.

2. Problem formulation and numerical model

2.1. Problem formulation

There are many issues that need to be addressed in the selection of a numerical model that can be used to simulate the flow over gabion stepped spillways (Fig. 1) such as the model's capability to simulate the turbulent flow over the porous media, the treatment of the interface between the fluid layer and porous medium, and the treatment of the free surface. Since this study mainly aimed to investigate the location of the inception point, many cases have been tested in order to assess the inception point location under different flow conditions, step heights, and spillway slopes with wide ranges of gabion stone sizes and porosity. The inception point determines the endpoint of the non-aerated zone; this point is immediately followed by the aerated zone. Air entrainment is one of the most important factors that can protect the hydraulic structures from cavitation damage due to the air-water flow. The inception point is defined as the point where the boundary layer intersects the free surface. The boundary layer thickness can be predicted by determining the point where the velocity is 99% of its maximum value in the velocity distribution profile at any particular location along the spillway (Schlichting, 1979; Husain et al., 2013). Thus, the water depth at that point, measured perpendicular to the pseudo-bottom, can be obtained directly from the computed values of the free surface.

2.2. Numerical model

As the flow in this study contained elements that were subcritical, supercritical, and highly turbulent, we used a code that solved the Reynolds-averaged Navier-Stokes (RANS) equations with a turbulence sub-model. The code chosen was NEWFLUME, described in detail by Lin and Xu (2006), which solves the RANS equations in two dimensions (2DV). For completeness' sake, we provide a brief description of the equations and solution technique here. The equations for flow outside the porous media are

$$\frac{\partial \overline{u_i}}{\partial x_i} = 0 \tag{1}$$

$$\frac{\partial \overline{u_i}}{\partial t} + \overline{u_j}\frac{\partial \overline{u_i}}{\partial x_j} = -\frac{1}{\rho}\frac{\partial \overline{P}}{\partial x_i} + g_i + \frac{1}{\rho}\frac{\partial}{\partial x_j}\left(\mu\frac{\partial \overline{u_i}}{\partial x_j} - \rho\overline{u_i'u_j'}\right) \tag{2}$$

where $\overline{u_i}$ is the mean velocity in the x_i direction ($i = 1$ means the horizontal direction, and $i = 2$ means the vertical direction) (m/s), t is time (s), $\overline{P}$ is the mean pressure (kN/m^2), ρ is the fluid density (kg/m^3), g_i is the gravitational acceleration in the x_i direction (m/s^2), μ is the molecular viscosity (kg/(m•s)), and $\overline{u_i'u_j'}$ represents the Reynolds stress (kN/m^2).

The mean viscous stress is written as

$$\overline{\tau_{ij}} = \mu\frac{\partial \overline{u_i}}{\partial x_j} + \mu\frac{\partial \overline{u_j}}{\partial x_i} \tag{3}$$

The Reynolds stress was calculated using a nonlinear eddy viscosity model. This model used mean velocity, turbulence kinematic energy (k), and dissipation rate of turbulence (ε). The k-ε transport equation was used to calculate k and ε (Lin and Xu, 2006).

The mean flow in the porous media is governed by

$$\frac{\partial \overline{u_i^*}}{\partial x_i} = 0 \tag{4}$$

$$\frac{1 + C_A}{n}\frac{\partial \overline{u_i^*}}{\partial t} + \frac{\overline{u_j^*}}{n^2}\frac{\partial \overline{u_i^*}}{\partial x_j} = -\frac{1}{\rho}\frac{\partial \overline{P}}{\partial x_i} + g_i + \frac{\nu}{n}\frac{\partial^2 \overline{u_i^*}}{\partial x_j \partial x_i} - ga_P\overline{u_i^*} - gb_P\sqrt{\overline{u_k^*}\,\overline{u_k^*}}\,\overline{u_i^*} \tag{5}$$

where $\overline{u_i^*}$ is the mean velocity in the x_i direction (m/s); n is the porosity of the porous medium; ν is the kinematic viscosity (m^2/s); g is the gravitational acceleration (m/s^2); C_A, a_P, and b_P are the coefficients of the porous medium; and the subscript k refers to the summation of velocities in the two directions.

The coefficients in Eqs. (4) and (5) are given by Lin and Xu (2006) as

$$C_A = \gamma_P\frac{1-n}{n}$$

$$a_P = \alpha\frac{(1-n)^2}{n^3}\frac{\nu}{gD_{50}^2}$$

$$b_P = \beta\left(1 + \frac{7.5}{K_C}\right)\frac{1-n}{n^3}\frac{1}{gD_{50}^2}$$

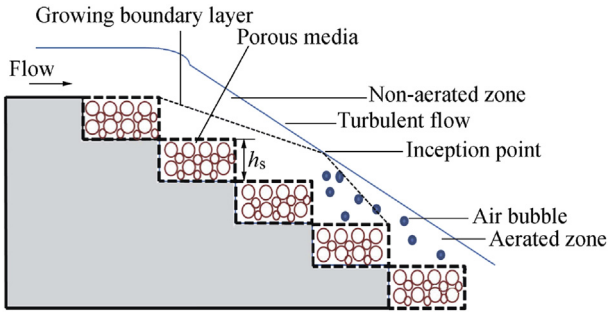

Fig. 1. Turbulent flow over gabion stepped spillway.

where D_{50} is the median diameter of gravel filling the gabions, $\gamma_P = 0.34$, $\alpha = 200$, $\beta = 1.1$, and $K_C = \sqrt{\overline{u_k^*}\,\overline{u_k^*}}T/(nD_{50})$, with T being a calibration parameter.

Free surface tracking was achieved through the application of the volume of fluid (VOF) method, which was originally established by Hirt and Nichols (1981) and subsequently adjusted by Kothe et al. (1991). A finite difference method was employed to approximate all partial differential equations. The calculation of the mean flow outside the porous media was performed with the Navier-Stokes equation solver that was developed by Kothe et al. (1991). This method used a two-step projection to solve the momentum equations. Initially the velocity was estimated without the pressure gradient term. In the second step the velocity was corrected using the updated pressure field, which was determined from the Poisson pressure equation. The governing equations for the flow through the porous media had the same structure as the RANS equations. However, Reynolds stresses were replaced by linear and nonlinear friction terms. The two-step projection technique was also used for the flow calculation through the porous media. On the interface between the porous media and outside flow, the continuity of the pressure and velocity was satisfied. The central difference method was used to discretize all the pressure and stress gradients in the projection method. The upwind scheme was combined with the central difference method to discretize the advection terms for the k-ε transport equation.

2.3. Sample validation

The capability of NEWFLUME was demonstrated by Lin and Xu (2006) through a series of case studies encompassing a wide range of turbulent free surface flows, covering coastal and ocean engineering (e.g., breaking wave interaction with a seawall and wave forces on a submerged pipeline), hydraulic engineering (e.g., dam break flow and hydraulic jump), and environmental modelling (e.g., jets and pollutant transport).

As an additional validation exercise for the case of flow down a gabion stepped spillway, we compared the model results against the experimental work of Wüthrich and Chanson (2014). Their test section consisted of a broad crested weir with a length of 1.01 m and a height of 1.0 m, followed by ten identical impervious steps with a height of 0.1 m and a length of 0.2 m. Gabion steps were installed over the impervious steps, which were made from marine plywood, with a 0.1-m height and a 0.3-m length. Gravel inside the gabions had a D_{50} of 0.01 m. The porosity ranged from 0.35 to 0.40.

The same experimental conditions were established in the numerical model. The mesh sizes were set to 0.010 m and 0.005 m in the x- and y-directions, respectively. The initial water depth was set to 1.4 m in order to achieve a required discharge. The discharge was calculated by determining the critical section over the broad crested weir. The critical section was determined by testing directly, from the model output, the value of the Froude number, Fr, with $Fr = q/\sqrt{gh^3}$, where q is the discharge per unit width, and h is the water depth. The critical section occurred where $Fr = 1$. To ensure numerical stability, the initial time step was set to 0.001 s and the simulated period was 24 s. As in the laboratory experiments, all of the boundaries were closed except the right boundary, which was open. It is important to mention that dam break conditions were used in the numerical model rather than the steady state used in the experiments of Wüthrich and Chanson (2014). Dam break conditions were used in order to capture different values of discharge at different times and also to observe the development of the flow pattern, such as nappe flow, transient flow, and skimming flow, over the gabion boxes. In the numerical model, dam break conditions were recreated with the fluid at rest and an impermeable barrier placed at $x = 9.0$ m, as shown in Fig. 2, in which velocity vectors are plotted at regular grid points to give an indication of the fluid layer, free surfaces are contoured in blue continuous lines, the outline of the impermeable dam is shown as black lines, and gabion steps are shown as red lines. This barrier was removed instantaneously at $t = 0$ s and the fluid then moved under the force of gravity.

The porosity of gravel was set equal to 0.375, representing the average value used in the experimental study. The fluid was initially at rest. The volume of the upstream tank was 9.0 m × 1.4 m per unit width. The barrier at $x = 9.0$ m was removed instantaneously and the resulting flow was computed (Fig. 2). The validation was conducted in terms of the location of the inception point. The velocity distribution over the outer edge of the steps was used to determine the inception point. As illustrated in Fig. 3, the velocity profile over the steps in the non-aerated zone is quasi-parabolic with no quasi-uniform segment in the upper part of the flow profile. The physical meanings of the variables in Fig. 3 can be found in Section 3.3.

Results shown in Table 1 illustrate that the model was able to simulate the flow over the gabion steps and also to capture the location of the inception point in agreement with experimental results. Further details of the validation testing can be found in Zuhaira et al. (2017).

3. Results and discussion

3.1. Model set-up

In the numerical model, two arrangements were used to accommodate the spillway geometry variations described in Section 3.2 and to meet the requirement that the critical water depth be established over the weir crest. For the spillway with 0.06-m-high steps, the weir was placed at $x = 6.9$ m, while for spillways with step heights of 0.09 m and 0.12 m, the weir was placed at $x = 7.4$ m. In all cases the length of the weir crest was set to 0.6 m.

The initial water depths were 1.58 m, 1.70 m, and 1.80 m for spillways with step heights of 0.12 m, 0.06 m, and 0.09 m, respectively, which ensured that the upstream tank contained sufficient water to achieve the required discharge and also to mitigate the effects of transients. The total simulation time was set to 15.0 s for the 0.12-m step height, 16.5 s for the 0.09-m

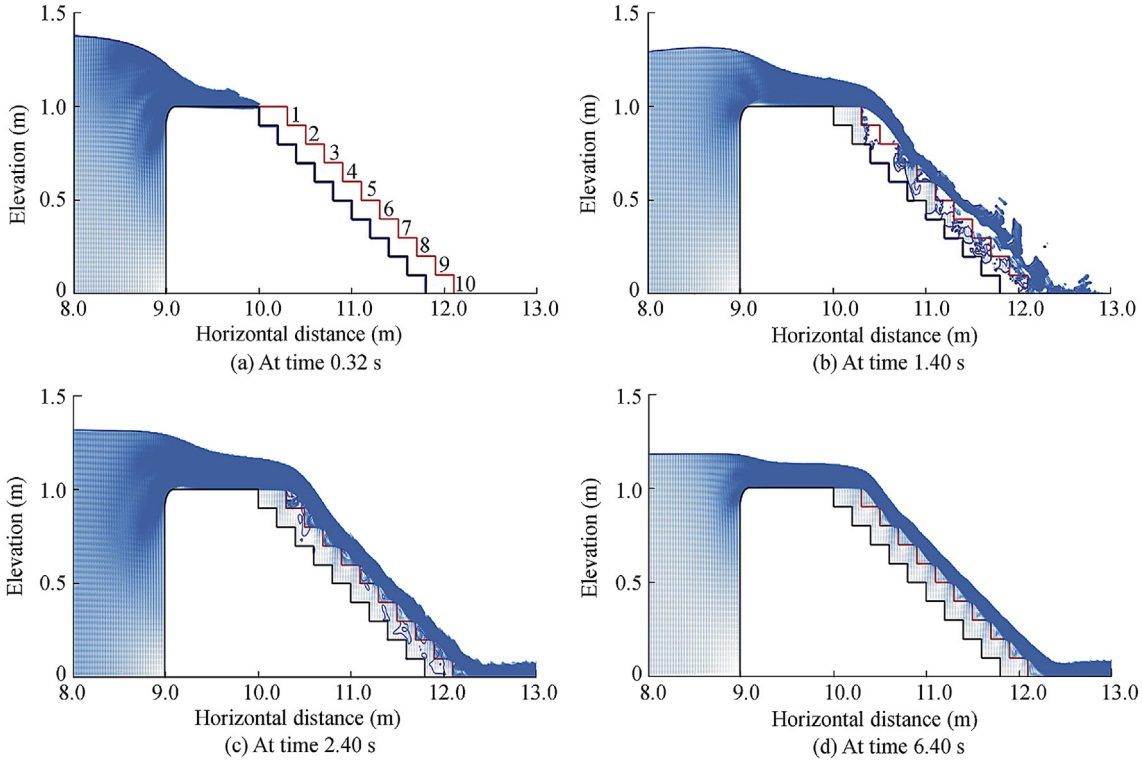

Fig. 2. Flow over gabion stepped spillway at different times.

step height, and 18.0 s for the 0.06-m step height. The time step was set at 0.0001 s to satisfy the stability criterion in all cases. The mesh sizes in the *x*- and *y*-directions were 0.010 m and 0.005 m, respectively for 0.09-m and 0.12-m step heights. However, for the 0.06-m step height, they were reduced to 0.0075 m in the *x*-direction and 0.0030 m in the *y*-direction, respectively. The model domain had closed boundaries except for the right-hand boundary, which was set as an open boundary to let the water exit the flume. Overall, many cases of gabion stepped spillways were tested in the current study. Each step height (0.12, 0.09, and 0.06 m) was examined individually with three spillway slopes (1:2, 1:2.5, and 1:3). Then, for each of these nine spillway geometries, simulations were performed for four different gravel sizes and four different values of porosity. A step height of 0.12 m with a 1:2 spillway slope was chosen initially in order to test the selected gravel sizes and porosity. Comparisons were conducted for specific discharges at the skimming flow stage.

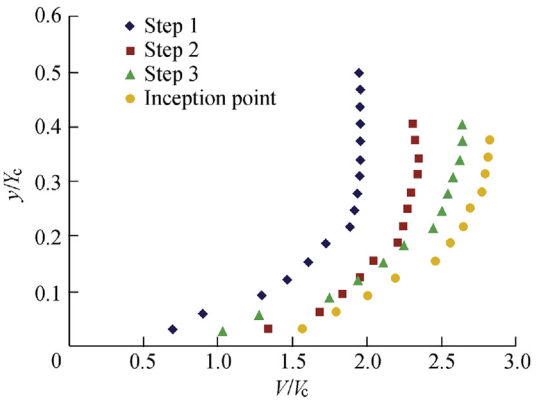

Fig. 3. Velocity distribution over different steps in non-aerated zone.

Parameter values of typical gravel were used to represent the porous media component. According to the standards, the minimum diameter of particles should be greater than 2 mm in order to consider them gravel (Wentworth, 1922). Therefore, the minimum value for the gravel size in this study was set to 5 mm. The diameters of 10 mm, 15 mm, and 20 mm were tested as well. The porosity of gravel normally ranges between 0.25 and 0.40. Therefore, values of 0.25, 0.30, 0.35, and 0.40 were tested in this study.

To summarize, a set of numerical experiments were conducted to compute the flow over gabion stepped spillways for a dam break case in which the step height, spillway slope, gravel diameter, gravel porosity, and gabion geometry varied individually.

Table 1
Comparison between inception point locations of experimental and numerical results.

Time (s)	Discharge per unit width (m^2/s)	Inception point location	
		Wüthrich and Chanson (2014)	Numerical model
5.57	0.11	Step 8 to step 9	At outer edge of step 8
5.98	0.10	Step 7 to step 8	At outer edge of step 7
6.43	0.08	Step 5 to step 6	At outer edge of step 5
7.01	0.06	Step 5	At middle of step 5

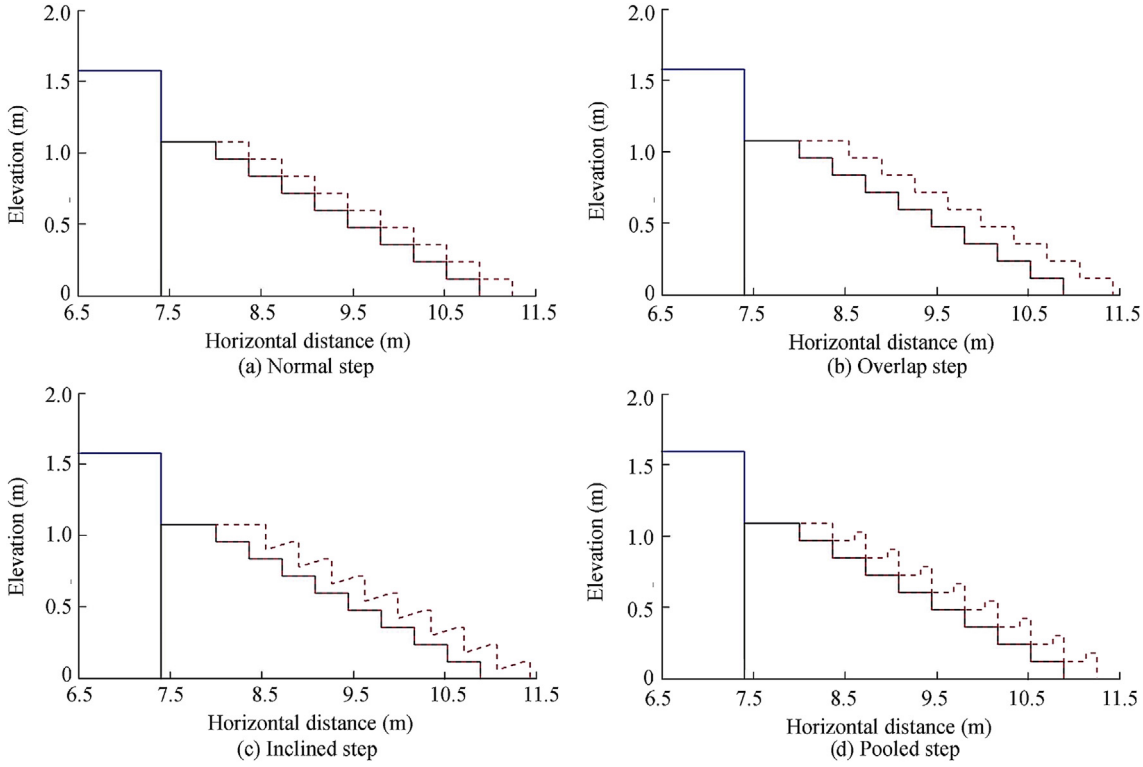

Fig. 4. Four different configurations of gabion steps considered in this study.

3.2. Different step geometries

The four different gabion step geometries, normal, overlap, inclined, and pooled, are shown in Fig. 4 for the case in which the step height was 0.12 m. All the configurations of the gabion steps were installed over impervious steps. The same initial conditions were applied in all configurations in order to determine the differences in terms of the time to establish skimming flow, the location of the inception point, and energy dissipation.

3.3. Energy dissipation

Energy dissipation is one of the most important parameters from the hydraulic design point of view. To investigate the energy dissipation for each of the gabion configurations, we applied Bernoulli's equation, following Husain (2013). The variables required to estimate the energy dissipation are described in Fig. 5, where P is the pressure head at the top of the weir (m). The datum, or zero head line, is shown as a dashed horizontal line, and the total head is demonstrated by a full horizontal line at the top of the figure. In brief, two points are required to determine the energy dissipation (ΔH). At the first point (a point under consideration in the non-aerated zone), the head H is calculated as follows:

$$H = y\cos\theta + \frac{aV^2}{2g} \tag{6}$$

where y is the perpendicular depth of water over a pseudo-bottom (m), tan θ is the spillway slope, a is the energy coefficient (unitless), and V is the fluid velocity (m/s).

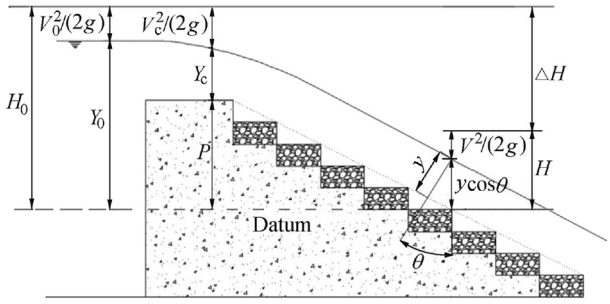

Fig. 5. Two-dimensional schematic view of stepped spillway showing parameters required to estimate residual energy at outer edge of steps.

The second point is located upstream of the weir and the head is calculated as

$$H_0 = Y_0 + \frac{V_0^2}{2g} \tag{7}$$

where Y_0 is the flow depth above the horizontal surface of the step under consideration (m), and V_0 is the approach flow velocity (m/s).

Hence, as shown in Fig. 5, the total energy dissipation with respect to the point under consideration is

$$\Delta H = H_0 - H \tag{8}$$

The computational results of energy dissipation at $x = 9.44$ m were 0.099, 0.076, 0.069, and 0.046 m^2/s^2 for the spillways with normal, overlap, inclined, and pooled gabion steps, respectively. This demonstrates that for this situation

normal gabion steps had the best performance in terms of energy dissipation, while pooled gabion steps exhibited the worst performance. To investigate this, further calculations of the turbulent kinetic energy (TKE) of the flow were made. TKE is the kinetic energy per unit mass of the turbulent fluctuation in the flow. It is generally accepted that, for spillway flow, the energy dissipation induced by turbulent eddies is greater than the energy loss due to internal and boundary frictions. Thus, there is a strong relation between the energy dissipation and TKE, and overall energy dissipation is prompted by creating turbulent flow (Husain, 2013).

The TKE was computed directly from the instantaneous velocities over the whole domain (see Fig. 6(a)). The plot shows that, from being initially at rest, the fluid gradually accelerates down the spillway, resulting in a rise in TKE as the discharge changes from nappe to transition to skimming flow. There are some fluctuations in TKE as skimming flow is established during the time between 2 s and 4 s after the dam break, and then TKE gradually decreases as the head in the upstream tank falls towards the level of the weir.

The results reveal that normal gabion steps generated greater amounts of TKE, by inference greater overall energy dissipation, than the other shapes. The finding is in agreement with the calculated results of energy dissipation for different gabion geometries. For all the gabion geometries, there is a slight increase in TKE for 7.5 s $< t <$ 8.5 s, arising from an increase in the discharge at this time due to the reflected transient in the upstream tank. Finally, as a further check, the turbulent energy dissipation rate, ε, calculated directly from the k-ε equation, is shown in Fig. 6(b), and confirms that the turbulent kinetic energy and its dissipation rate have a similar morphology over time.

3.4. Inception point location

The computational results of the inception point location were 9.75, 10.16, 10.20, and 10.32 m from the downstream edge of the weir for the spillways with normal, overlap, inclined, and pooled gabion steps, respectively. The results show that the non-aerated zone for normal gabion steps was smaller than those for other types of gabion steps, while the longest non-aerated zone was observed for pooled gabion steps. Also, the results show that there was a small difference between overlap gabion steps and inclined gabion steps in terms of the inception point location. Normal gabion steps exhibited the best results in terms of energy dissipation and the location of inception point.

3.5. Sensitivities to slope, porosity, and gravel size

As the normal step configuration exhibited the best performance in terms of energy dissipation, discussion in this section is restricted to this case. Three different step heights and three different step widths for a given weir height were tested with the numerical code to investigate the impact of step configuration on the flow properties over gabion stepped spillways. Step widths were set to give spillway slopes of 1:2, 1:2.5, and 1:3. The porosity of the gabion steps was varied from 0.25 to 0.40, while the gravel sizes were varied from 0.005 m to 0.020 m. The selection of these values provided wide-ranging physical characteristics likely to be encountered in real schemes in order to investigate the effects of the gabion porosity, gabion gravel size, spillway slope, and step height on the flow characterization.

Fig. 7 shows the effect of the step height on the location of the inception point. The calculations of the developing boundary layer thickness were carried out at the end of each step, in order to determine the location of the inception point. In the plot, the dots denote the top of the boundary layer at the end of each step, and the inception point occurs where the boundary layer meets the free surface that is shown as the blue line. It is clear that step heights affect the location of the inception point and the length of the non-aerated zone.

The location of the inception point moves downslope as the discharge increases. In other words, the length of the non-aerated zone increases with the flow rate. This is most likely related to the discharge, as increasing discharges imply increases in flow depth and/or velocity. Increasing the flow depth might increase the length of the boundary layer required to intersect the free surface profile. For a given slope and discharge, it is observed that the location of the inception point moves to the upstream side towards the weir crest when the

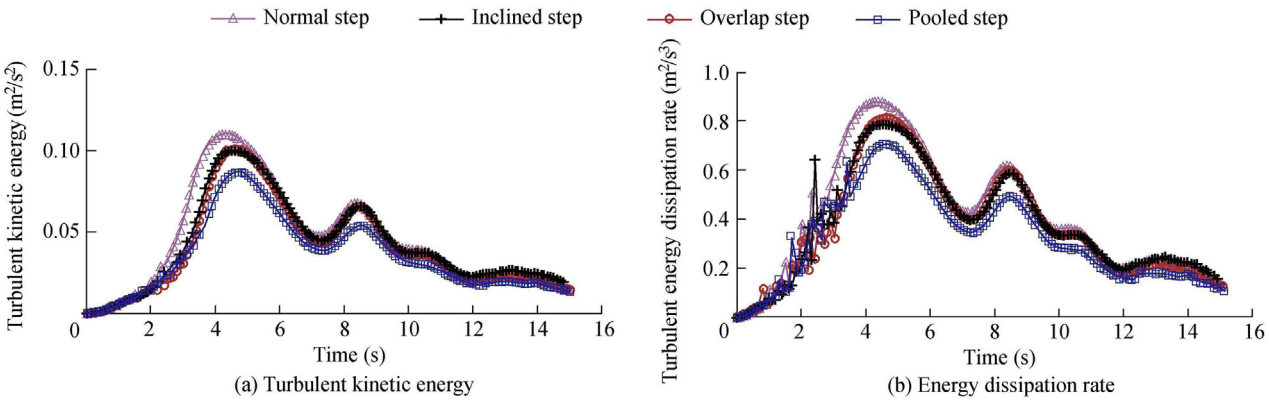

Fig. 6. Turbulent kinetic energy and its dissipation rate for different gabion geometries.

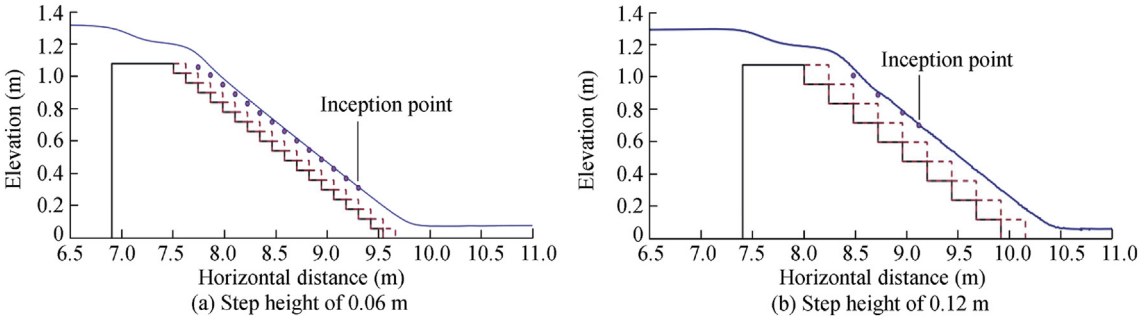

Fig. 7. Estimation of inception point location for spillway slope of 1:2 and unit discharge equal to 0.2 m^2/s.

step height is increased (Fig. 7). This can be attributed to the fact that large step heights can have a stronger impact on the location of the inception point than small step heights as the velocity of the overflowing water is decelerated when it flows over the outer step edge and hits the horizontal face. However, this effect might be expected to decrease with lesser discharges.

In order to investigate the effect of the spillway slope on the location of the inception point and the length of the non-aerated zone, three different slopes (1:2, 1:2.5, and 1:3) were tested with three different step heights (0.06, 0.09, and 0.12 m). Three values of discharge, 0.25, 0.20, and 0.15 m^2/s, were used for comparison purposes to explore how the discharge influences the results.

The general trend of the numerical results reveals that the location of the inception point may move upslope when the spillway slope becomes steeper. Therefore, it can be concluded that the length of the non-aerated zone has a reciprocal dependence on the spillway slope (Fig. 8). In other words, a shorter length of the non-aerated zone will be expected for a steep spillway slope in comparison with a flat spillway slope. This can be explained by the fact that the longitudinal velocity over steep slopes is higher than that over flat slopes. Therefore, the flow depth will be lower for steep spillway slopes. This is likely to accelerate the development of the boundary layer and its expansion throughout the water column to meet the free surface. All of the previous observations agree with the experimental observation of André (2004) who conducted a study on normal stepped spillways. However, for gabion stepped spillways, this kind of relation has not been reported before.

Furthermore, the results show that both porosity and gravel size can have a significant impact on the location of the inception point. The computational results for high discharges reveal a general trend that, when the gravel size decreases, the location of the inception point moves upslope towards the weir. Thus, the length of the non-aerated zone will be shorter. A relationship between porosity, gravel size, and the length of the non-aerated zone seems stronger for larger discharges. To quantify the relationship, we describe a nonlinear multiple regression analysis in the next section to determine the strength and robustness of the putative relationships discussed above.

3.6. Predictive formulae

Previous studies such as Chanson (1996), Carosi and Chanson (2008), Meireles and Matos (2009), Hunt and Kadavy (2011), and Husain et al. (2013) have developed nonlinear multiple regression equations to fit the results obtained in their work for normal stepped spillways to predict the length of the non-aerated zone and the water depth at the inception point. Our computational results were compared with the results from those nonlinear multiple regression equations. Some deficiencies were observed which provided the motivation to develop modified formulae appropriate for gabion stepped spillways. For this purpose, the values of the length of the non-aerated zone, L_i, and the corresponding

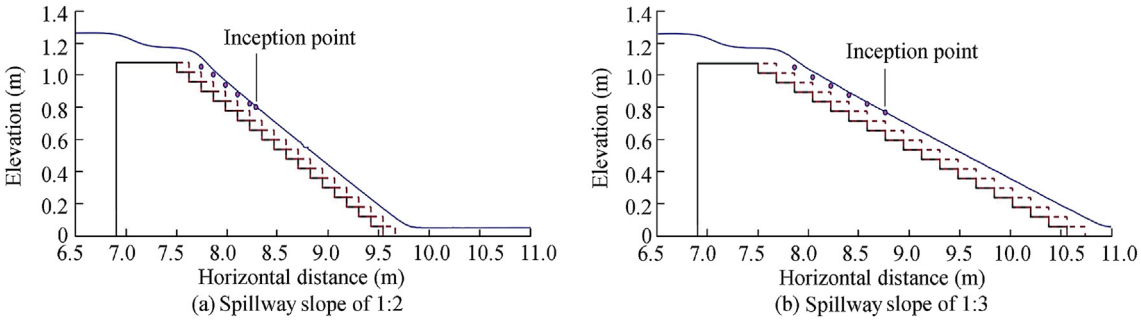

Fig. 8. Estimation of inception point location for 0.06-m step height and unit discharge equal to 0.15 m^2/s.

values of the roughness Froude number, F_*, collected from the cases described above were used to obtain the following relationship:

$$\frac{L_i}{k_s} = 2.2281(\sin\theta)^{-0.3172} F_*^{1.2486} n^{-0.2831} \left(\frac{D_{50}}{h_s}\right)^{0.1537} \quad (9)$$

where k_s is the roughness, which is calculated as $h_s \cos\theta$, and h_s is the step height. The roughness Froude number can be calculated from

$$F_* = \frac{q}{\sqrt{g \sin\theta k_s^3}} \quad (10)$$

In developing Eq. (9), we started with Chanson's (1994) equation for normal stepped spillways and included extra terms related to gabion boxes. The coefficients of Eq. (9) were estimated using an iterative least squares estimation routine available in MATLAB. For the fitting, results from the computational model were split into two groups. The first group, which contained around 80% of the data, was used to find the coefficients of the equation. The remaining data (20%) were used to test the equation. All the data were selected randomly and were restricted to cases in which the step geometry was normal. The coefficient of determination, R^2, was used to measure how well the regression line approximated the data. If the value of R^2 approached 1.00, then the regression line was considered to have provided a perfect representation of the data. Fig. 9 shows that the value of R^2 for Eq. (9) is 0.9057, with a correlation factor of 0.952, which gives an indication that the formula describes the data well.

The regression analysis indicates that the porosity term has a negative power sign, which reveals a reciprocal relationship between porosity and the length of the non-aerated zone. Also, a small value for the power, which is −0.2831, suggests that porosity has less impact on the length of the non-aerated zone than either F_* or the spillway slope. The positive exponent for the gravel size shows a direct relationship between the gravel size and the length of the non-aerated zone, and again the value is quite small, which means that the dependence of L_i on the gravel size is not very strong.

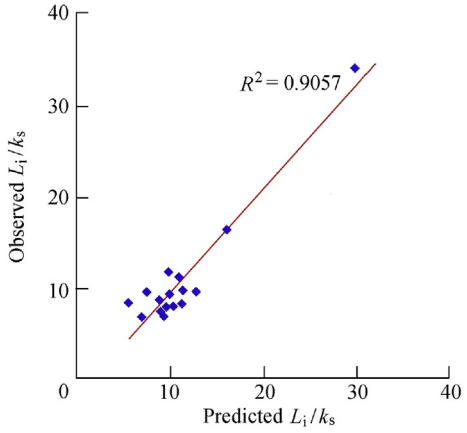

Fig. 9. Data test against Eq. (9).

A further comparison was conducted against different empirical equations for normal stepped spillways, including (1) $L_i/k_s = 9.8(\sin\theta)^{0.08} F_*^{0.71}$ from Chanson (1994), (2) $L_i/k_s = 1.05 + 5.11F_*$ from Carosi and Chanson (2008), (3) $L_i/k_s = 5.25F_*^{0.95}$ from Meireles and Matos (2009), (4) $L_i/k_s = 6.1(\sin\theta)^{0.08} F_*^{0.86}$ from Hunt and Kadavy (2011), and (5) $L_i/k_s = 5.19F_*^{0.89}$ from Hunt and Kadavy (2013). The objective of this comparison was to assess whether the empirical equations established for normal stepped spillways could be used to find the location of the inception point over gabion stepped spillways.

Comparisons of the predictions from these five formulae against the computational results of the present study are shown in Fig. 10. It is evident that all the formulae overestimate the location of the inception point in comparison with the computational results of the present study, with the formula from Hunt and Kadavy (2013) showing the closest agreement.

It is important to mention that the formulae from these earlier studies were derived from experimental results based on physical models of normal stepped spillways. However, the formula of the current study is based on the results of computational modelling. The results in Fig. 10 show that using gabion boxes increased the roughness of the spillway surface and therefore accelerated the growth of the boundary layer thickness. Hence, the length of the non-aerated zone was reduced. Using the formulae for normal stepped spillways to predict the non-aerated length over gabion stepped spillways will likely give an overestimation, leading to very conservative designs.

The computational results were used to develop another equation for estimation of the water depth at the inception point for gabion stepped spillways. The expression is given as follows:

$$\frac{D_i}{k_s} = 0.2569(\sin\theta)^{0.1175} F_*^{0.7469} n^{-0.1188} \left(\frac{D_{50}}{h_s}\right)^{-0.0091} \quad (11)$$

where D_i is the water depth at the inception point. Using the same procedure as that for development of Eq. (9), the values of R^2 and the correlation factor for Eq. (11) were obtained as 0.9413 and 0.97, respectively.

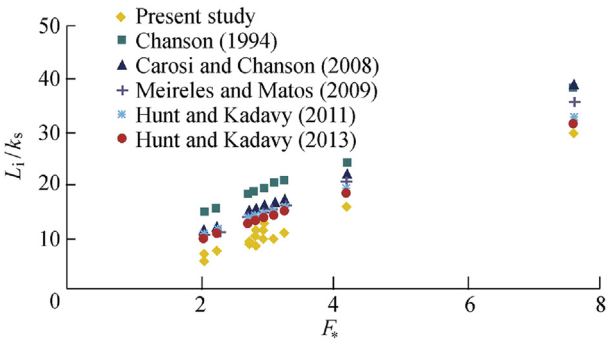

Fig. 10. Comparison of computational results against published formulae for length of non-aerated zone.

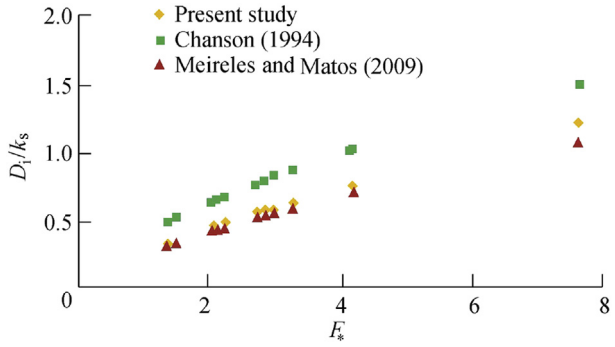

Fig. 11. Comparison of computational results against published formulae for water depth at inception point.

The results of Eq. (11) were compared with those of empirical formulae, i.e., $D_i/k_s = [0.4/(\sin\theta)^{0.04}]F_*^{0.64}$ from Chanson (1994) and $D_i/k_s = 0.28F_*^{0.68}$ from Meireles and Matos (2009), as shown in Fig. 11. Both of the empirical formulae were developed for normal stepped spillways, not for gabion stepped spillways. As can be seen in Fig. 11, the formula from Chanson (1994) consistently overestimates the water depth, while the formula of Meireles and Matos (2009) slightly underestimates the water depth, in comparison with the computational results of the present study.

It should be noted that both Eqs. (9) and (11) are valid for gabion stepped spillways. Both of the equations were obtained from the computational results for different step heights of 0.06, 0.09, and 0.12 m ($0.832 \leq Y_c/h_s \leq 3.080$) with different spillway slopes of 1:2, 1:2.5, and 1:3. Moreover, these equations were applicable for porosity ranging from 0.25 to 0.40 and D_{50} in the range of 0.005−0.020 m. The maximum discharge used was 0.25 m^2/s. As ever with empirically derived formulae, application outside the parameter ranges used to develop the formulae is not recommended unless further tests are performed.

4. Conclusions

The hydraulic performance of different gabion stepped spillways has been investigated with a state-of-the-art numerical model based on solving the RANS equations. To test the capability of the numerical model, a validation was conducted using the experimental data of Wüthrich and Chanson (2014). Four different geometries of gabion steps were investigated to compare the results in terms of energy dissipation and the location of the inception point. These four geometries were normal gabion steps, overlap gabion steps, inclined gabion steps, and pooled gabion steps.

The results showed different hydraulic characteristics for the four types of gabion steps in terms of energy dissipation and the inception point location. The normal gabion step geometry showed the best performance for the energy dissipation and the location of the inception point. The length of the non-aerated zone was explored for a range of step heights, spillway slopes, gabion porosity, and gabion gravel sizes using a computational model. The results showed that the length of the non-aerated zone increased with decreasing step height and also with decreasing spillway slope. A weaker dependence of the location of the inception point on both porosity and gravel size was found.

Two empirical equations were derived on the basis of the regression analysis to estimate the location of the inception point and the water depth. These two equations were compared with other formulae developed on the basis of physical experiments for the flow over normal stepped spillways. The results showed that using gabion boxes would increase the roughness of the spillway surface and therefore accelerate the growth of the boundary layer thickness. It would further reduce the length of the non-aerated zone. Overall, using porous media over concrete steps, as simulated in this study, would be expected to reduce the non-aerated length and thus reduce the danger of cavitation damage over the steps.

References

André, S., 2004. High Velocity Aerated Flows on Stepped-chutes with Macro-roughness Elements, Communication 20. Laboratorie de Constructions Hydrauliques, École Polytechnique Fédérale de Lausanne, Lausanne.

André, S., Schleiss, A., 2004. High Velocity Aerated Flows on Stepped Chutes with Macro-roughness Elements. École Polytechnique Fédérale de Lausanne, Lausanne. https://doi.org/10.5075/epfl-thesis-2993.

Boes, R.M., Hager, W.H., 2003. Hydraulic design of stepped spillways. J. Hydraul. 129(9), 671−679. https://doi.org/10.1061/(ASCE)0733-9429(2003)129:9(671).

Carosi, G., Chanson, H., 2008. Turbulence characteristics in skimming flows on stepped spillways. Can. J. Civ. Eng. 35(9), 865−880. https://doi.org/10.1139/L08-030.

Chanson, H., 1994. Hydraulics of skimming flows over stepped channels and spillways. J. Hydraul. Res. 32(3), 445−460. https://doi.org/10.1080/00221689409498745.

Chanson, H., 1995. Air Bubble Entrainment in Free-Surface Turbulent Flows: Experimental Investigations, Report CH46/95. University of Queensland, Queensland.

Chanson, H., 1996. Prediction of the transition nappe/skimming flow on a stepped channel. J. Hydraul. Res. 34(3), 421−429. https://doi.org/10.1080/00221689609498490.

Chanson, H., 2002. The Hydraulics of Stepped Chutes and Spillways. A. A. Balkema Publishers, Lisse.

Chinnarasri, C., Donjadee, S., Israngkura, U., 2008. Hydraulic characteristics of gabion-stepped weirs. J. Hydraul. Eng. 134, 1147−1152. https://doi.org/10.1061/(ASCE)0733-9429(2008)134:8(1147).

Freeman, G.E., Fischenich, J.C., 2000. Gabions for Streambank Erosion Control, EMRRP Technical Notes Collection (ERDC TN-EMRRP SR-22). U.S. Army Engineering Research and Development Center, Vicksburg.

Hirt, C.W., Nichols, B.D., 1981. Volume of fluid (VOF) method for the dynamics of free boundaries. J. Comput. Phys. 39(1), 201−225. https://doi.org/10.1016/0021-9991(81)90145-5.

Hunt, S.L., Kadavy, K.C., 2011. Inception point relationship for flat-slopped stepped spillways. J. Hydraul. Eng. 137(2), 262−266. https://doi.org/10.1061/(ASCE)HY.1943-7900.0000297.

Hunt, S.L., Kadavy, K.C., 2013. Inception point for embankment dam stepped spillway. J. Hydraul. Eng. 139(1), 60−64. https://doi.org/10.1061/(ASCE)HY.1943-7900.0000644.

Husain, S.M., 2013. Computational Investigation of Skimming Flow on Stepped Spillways Using the Smoothed Particle Hydrodynamics Method. Ph. D. Dissertation. Swansea University, Swansea.

Husain, S.M., Muhammed, J.R., Karunarathna, H.U., Reeve, D.E., 2013. Investigation of pressure variation over stepped spillways using smooth particle hydrodynamics. Adv. Water Resour. 66, 52−69. https://doi.org/10.1016/j.advwatres.2013.11.013.

Kells, J.A., 1994. Energy dissipation at a gabion weir with throughflow and overflow. In: Proceedings of Annual Conference of the Canadian Society for Civil Engineering. Canadian Society for Civil Engineering, Winnipeg, pp. 1−4.

Kothe, D.B., Mjolsness, R.C., Torrey, M.D., 1991. RIPPLE: A Computer Program for Incompressible Flows with Free Surface, Rep. LA-12007-MS. Los Alamos National Laboratory, Los Alamos.

Lin, P., Xu, W., 2006. NEWFLUME: A numerical water flume for two two-dimensional turbulent free surface flow. J. Hydraul. Res. 44(1), 60−64. https://doi.org/10.1080/00221686.2006.9521663.

Manes, C., Pokrajac, D., McEwan, I., Nikora, V., 2009. Turbulence structure of open channel flows over permeable and impermeable beds: A comparative study. Phys. Fluids 21(12), 125109. https://doi.org/10.1063/1.3276292.

Meireles, I., Matos, J., 2009. Skimming flow in the non-aerated region of stepped spillways over embankment dams. J. Hydraul. Eng. 135(8), 685−689. https://doi.org/10.1061/(ASCE)HY.1943-7900.0000047.

Novak, P., Mofatt, A.I.B., Nalluri, C., Narayanan, R., 2001. Hydraulic Structures, fourth ed. Taylor and Francis, London and New York.

Novak, P., Guinot, V., Jeffrey, A., Reeve, D.E., 2010. Hydraulic Modelling: An Introduction. Spon Press, Abingdon.

Peyras, L., Royet, P., Degoutte, G., 1992. Flow and energy dissipation over stepped gabion weirs. J. Hydraul. Eng. 118(5), 707−717. https://doi.org/10.1061/(ASCE)0733-9429(1992)118:5(707).

Salmasi, F., Chamani, M.R., Zadeh, D.F., 2012. Stepped gabion spillways with low heights. IJST: Trans. Civ. Eng. 36(2), 253−264. https://doi.org/10.22099/ijstc.2012.640.

Schlichting, H., 1979. Boundary Layer Theory. McGraw-Hil, New York.

Stephenson, D., 1979. Gabion energy dissipators. In: Transactions of the 13th International Congress on Large Dams. International Commission on Large Dams, New Delhi, pp. 33−43.

Wentworth, C., 1922. A scale of grade and class terms for clastic sediments. J. Geol. 30(5), 377−392.

Wüthrich, D., Chanson, H., 2014. Hydraulics, air entrainment, and energy dissipation on a gabion stepped weir. J. Hydraul. Eng. 140(9), 04014046. https://doi.org/10.1061/(asce)hy.1943-7900.0000919.

Zhang, G., Chanson, H., 2014. Two-phase flow on a gabion stepped spillway: Cavity and seepage air-water motion. In: Proceedings of the 19th Australasian Fluid Mechanics Conference. Australasian Fluid Mechanics Society, Melbourne.

Zhang, G., Chanson, H., 2016a. Gabion stepped spillway: Interactions between free-surface, cavity and seepage flows. J. Hydraul. Eng. 142(5). https://doi.org/10.1061/(ASCE)HY.1943-7900.0001120.

Zhang, G., Chanson, H., 2016b. Hydraulics of the developing flow region of stepped spillways, Part I: Physical modelling and boundary layer development. J. Hydraul. Eng. 142(7). https://doi.org/10.1061/(ASCE)HY.1943-7900.0001138.

Zuhaira, A.A., Karunarathna, H.U., Reeve, D.E., 2017. Numerical investigation of step dimensions impact over gabion stepped spillways. In: Proceedings of the 37th IAHR World Congress. International Association for Hydro-Environment Engineering and Research, Kuala Lumpur.